Journal of Photochemistry and Photobiology A: Chemistry 200 (2008) 301–306

Contents lists available at ScienceDirect

Journal of Photochemistry and Photobiology A: Chemistry

journal homepage: www.elsevier.com/locate/jphotochem

TiO_2–carbon nanotube heterojunction arrays with a controllable thickness of TiO_2 layer and their first application in photocatalysis

Hongtao Yu, Xie Quan*, Shuo Chen, Huimin Zhao, Yaobin Zhang

Key Laboratory of Industrial Ecology and Environmental Engineering (Ministry of Education), School of Environmental and Biological Science and Technology, Dalian University of Technology, Dalian 116024, China

ARTICLE INFO

Article history:
Received 18 December 2007
Received in revised form 21 June 2008
Accepted 15 August 2008
Available online 26 August 2008

Keywords:
TiO_2
Carbon nanotube
Heterojunction
Photocatalysis

ABSTRACT

TiO_2–carbon nanotube (CNT) heterojunction arrays on Ti substrate were fabricated by a two-step thermal chemical vapor deposition (CVD) method. CNT arrays were first grown on Ti substrate vertically, and then a TiO_2 layer, whose thickness could be controlled by varying the deposition time, was deposited on CNTs. Measured by electrochemical impedance spectroscopy (EIS), the thickness of the TiO_2 layer could affect the photoresponse ability significantly. About 100 nm thickness of the TiO_2 layer proved to be best for efficient charge separation among the tested samples. The optimized TiO_2–CNT heterojunction arrays displayed apparently higher photoresponse capability than that of TiO_2 nanotube arrays which was confirmed by surface photovoltage (SPV) technique based on Kelvin probe and EIS. In the photocatalytic experiments, the kinetic constants of phenol degradation with TiO_2–CNT heterojunctions and TiO_2 nanotubes were 0.75 h^{-1} (R^2 = 0.983) and 0.39 h^{-1} (R^2 = 0.995), respectively. At the same time, 53.7% of total organic carbon (TOC) was removed with TiO_2–CNT heterojunctions, while the removal of TOC was only 16.7% with TiO_2 nanotubes. These results demonstrate the super capability of the TiO_2–CNT heterojunction arrays in photocatalysis with comparison to TiO_2-only nanomaterial.

1. Introduction

TiO_2 is by far the most widely studied photocatalytic material because of its high photocatalytic activity, long-term chemical stability, nontoxicity and low price [1]. The photocatalysis process involves ultraviolet (UV) light to excite an electron from the valence band of TiO_2 to its conduction band, leaving a hole to oxidize organics in water directly or indirectly [2]. However, this process with TiO_2 always suffers from the low quantum yield that is caused by the rapid recombination of photogenerated electrons and holes [3].

It is well known when a semiconductor is constructed a heterojunction with other semiconductors or metals, a space charge layer ranging from several tens to hundreds nanometers would be formed near the interface to make their Fermi level equal, thus the electrostatic force of space charge layer could separate photogenerated electrons and holes immediately if photogenerated electrons could diffuse into space charge layer. In a conventional photocatalytic system, the photogenerated electrons and holes migrate randomly and most of them recombine before they arrive at the photocatalyst surface. Whereas in a photocatalytic system involving heterojunction, the driving force which comes from interior electric field could separate electron–hole pairs efficiently, so the electrons and the holes would be driven to the different directions and the recombination could be reduced.

On the basis of this principle, nanoscale composites of TiO_2 with Pt [4], In_2O_3 [5], SnO_2 [6], WO_3 [7], SiO_2 and ZrO_2 [8], $CuAlO_2$ [9], Cu_2O [10] and Bi_2O_3 [11] have been fabricated to improve the photocatalytic ability. With the progress on carbon nanotubes (CNTs) research, CNTs have drawn the interest of a number of researchers due to their unique electrical property and high aspect ratio. Many endeavors were performed to develop nanocomposite materials of TiO_2 and CNTs by a sol–gel method in last decade, and enhanced photocatalysis abilities were obtained [12–14]. Nevertheless, the enhancement was still limited, because it is so difficult to disperse CNTs into the sol uniformly that many TiO_2 nanoparticles were far away from CNTs and some surfaces of CNTs were vacant and even shaded the light. On the other hand, most of the reported TiO_2-based composite materials were in powder form, which restricted their photocatalytic application because of the difficulty in separating them from aqueous solution. This problem could be overcome by immobilizing the powders on a solid substrate. Some works have been carried out to coat nonaligned CNTs with TiO_2 on solid substrates [15,16]. And recently, depositing TiO_2 on aligned CNTs using Si or SiO_2 as the substrates has been reported [17–19]. Although Si and SiO_2 are preponderant substrate materials for the growth of the CNT arrays, they are not suitable for investigating charge

* Corresponding author. Tel.: +86 411 84706140; fax: +86 411 84706263.
E-mail address: quanxie@dlut.edu.cn (X. Quan).

1010-6030/$ – see front matter © 2008 Elsevier B.V. All rights reserved.
doi:10.1016/j.jphotochem.2008.08.007

separation and transfer or photoelectrocatalytic ability because of CNTs scaling off from these substrates very easy together with the big connection resistances between CNTs and these substrates.

In our previous work, we have fabricated TiO_2–CNT arrays on Ti substrate, and studied their charge separation capability [20]. The TiO_2–CNT heterojunction arrays exhibited high photocurrent at zero bias potential, which demonstrated that the photogenerated charges were separated successfully owing to the firm and conductive connections between heterojunctions and Ti substrate. This TiO_2–CNT heterojunction arrays are expected good prospect in practical applications, especially in photocatalysis. Therefore, in present work we extended our research to explore the photocatalytic capability of the TiO_2–CNT heterojunction arrays and confirmed the super photocatalytic capability shown by the novel photocatalyst. Special attention has been paid to the relationship between charge separation efficiency and the thickness of TiO_2 layer because we believe that the thickness of TiO_2 layer is a key factor for efficient charge separation and photocatalysis of the heterojunction arrays.

2. Materials and methods

2.1. Fabrication of the heterojunction arrays

The fabrication of CNT arrays on Ti substrate was depicted in the reference [20]. After growing CNT arrays on Ti substrate at 800 °C, the system was allowed to cool down in argon. When the substrate temperature fell to 450 °C, the air was imported to remove amorphous carbon on the surface of CNTs. When the substrate cooled down continuously to an appropriate temperature, titanium (IV) isopropoxide (TTIP) was fed by a pump and swept into the reaction zone by an argon flow (1000 mL min^{-1}). After deposition, the substrate was annealed in air for 30 min to convert the amorphous phase TiO_2 to a crystalline one.

2.2. Characterization and measurements

The morphologies of the heterojunctions were characterized by environmental scanning electron microscopy (ESEM Quanta 200 FEG) and transmission electron microscopy (TEM FEI-Tecnai G^2 20). X-ray diffraction (XRD) was carried out on a Shimadzu XRD-6000 X-ray diffractometer with Cu Kα radiation (λ = 0.154060 nm) at a scanning speed of 0.02° s^{-1} in the 2θ range from 20° to 80°. Electrochemical impedance spectroscopy (EIS) were recorded by applying an AC voltage of 10 mV amplitude in the frequency range of 10^5 Hz to 10^{-2} Hz with the initial potential (0 V vs. a saturated calomel electrode (SCE)) in 0.01 M sodium sulfate using three-electrode cell that was connected to a CHI 650B electrochemical station (CH Instruments, Shanghai Chenhua, China), where the TiO_2–CNT arrays on Ti substrate acted as the working electrode, a platinum foil as the counter electrode and the SCE as the reference electrode. A 300-W high-pressure mercury lamp with a principal wavelength of 365 nm (Beijing Huiyixin Light, China) was used as the UV light source, and the light intensity was measured by a radiometer (model UV-A, Photoelectric Instrument Factory Beijing Normal University). Kelvin probe (KP)-based surface photovoltage (SPV) measurements were carried out on a commercial KP system (KP Technology Ltd., Scotland, UK). The width of the gold reference probe is 1.8 mm. A 500-W xenon lamp and a double prism monochromator provided monochromatic light, which was carefully focused on the sample below the probe. The SPV spectra were obtained by scanning the wavelength of the incident light over the visible and UV range (600–300 nm) with the rate of about 30 nm min^{-1}.

2.3. Photocatalytic experiment

Photocatalytic degradation of phenol in the aqueous solution (0.01 M sodium sulfate acted as the electrolyte) was carried out under a 300-W high-pressure mercury lamp irradiation in a reactor with a quartz window (2 cm × 2 cm) to allow the incident radiation to enter with minimal attenuation. The TiO_2–CNT heterojunction arrays serving as the photoanode and a platinum foil serving as the cathode were connected by a voltaic wire to transfer the photogenerated electrons from the photoanode to the cathode. For comparison, the TiO_2 nanotube arrays were prepared by the procedure described in Ref. [21] and they were used as the photoanode by replacing the TiO_2–CNT heterojunction arrays. The applied areas of both the CNT–TiO_2 heterojunctions and the TiO_2 nanotubes are 2 cm × 2 cm. The concentration of phenol was determined by high-performance liquid chromatography (HPLC, Waters 2695, Separations module) with a SunfireTM C18 (5 μm) reverse-phase column at 30 °C equipped with photodiode array detector (Waters 2996). The mobile phase was 0.5 mL min^{-1} of methanol and water (v:v = 0.55:0.45) and the wavelength was set at 280 nm for phenol and 254 nm for intermediates, respectively. Total organic carbon analyzer (TOC-V_{CPH}, Shimadzu, Japan) was employed for TOC determination.

3. Results and discussion

3.1. Thickness control of the TiO_2 layer

The thickness of the TiO_2 layer could be controlled by varying the deposition time. Fig. 1 illustrates the morphologies of TiO_2–CNT arrays with different TiO_2 deposition times. Observing from Fig. 1(a–d), the thickness of TiO_2 layer increased with the increase of deposition time. As shown in Fig. 1(e), the length of heterojunction array was about 4 μm, and the nanotubes were uniform in the axial direction except for their top, which was like a ball, and its diameter was bigger than that of the bottom nanotube. In order to estimate the thickness of the TiO_2 layer from the uniform parts, the details of TiO_2–CNT heterojunction nanotubes were distinguished in Fig. 2. For the TiO_2–CNT heterojunction with 5 min of TiO_2 deposition, a CNT wall and a TiO_2 layer about 10 nm were clearly seen in Fig. 2(a), and their lattice fringes were d = 0.34 and 0.35 nm, respectively, which matched those of the (0 0 2) crystallographic planes of graphitic sheets and the (1 0 1) crystallographic planes of anatase TiO_2. For the sample with depositing TiO_2 for 10 min, the total diameter of a heterojunction nanotube was obviously larger than that of the sample for 5 min and the boundary of CNT and TiO_2 could not be observed by TEM due to a thicker TiO_2 layer. However, it could be seen from a crack in a piece of TiO_2–CNT heterojunction nanotube in Fig. 2(b) that the diameters of CNT and TiO_2–CNT heterojunction nanotube were about 50 and 250 nm, respectively, so the thickness of TiO_2 layer was estimated about 100 nm. For the samples with 15 and 20 min of TiO_2 deposition, the thickness of TiO_2 layer was apparently much more than 100 nm.

Because TiO_2–CNT heterojunction arrays were grown on the conductive substrate, they could be used as electrode for investigation of photoelectrochemical properties. As a widely used electrochemical method, EIS is very effective to investigate the properties of the electron-transfer process across the TiO_2–electrolyte interfaces under light [22–24]. The less impedance arc radius in Nyquist plots indicates the faster electron transfer [25]. EIS measurements of TiO_2–CNT heterojunctions with different thickness of TiO_2 layer were performed to determine the optimal thickness for good charge separation, as shown in Fig. 3. The Nyquist plot of CNTs was almost a line with a big angle between the real

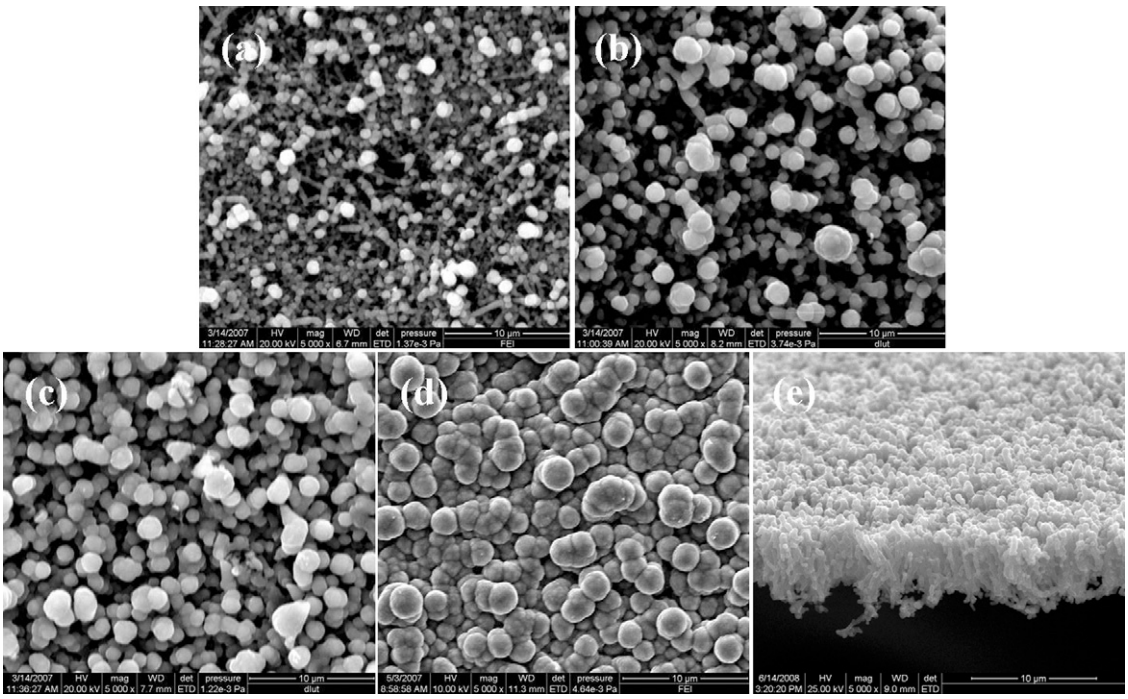

Fig. 1. SEM images of TiO_2–CNT heterojunction with depositing TiO_2 for different times: (a) 5 min, (b) 10 min, (c) 15 min, (d) 20 min and (e) profile of TiO_2–CNT heterojunction with depositing TiO_2 for 10 min.

axis, which indicated that the photoresponse of the CNTs could be ignored. From the Nyquist plots of samples after coating TiO_2, it was found that the size of the arc radius decreased with increasing thickness of TiO_2 layer in initial stage. After arriving at its minimum, the size of the arc increased with increasing thickness. These phenomena revealed that the thickness of the TiO_2 layer affected the electron transfer ability of the heterojunction significantly. Therefore, the thickness of the TiO_2 layer should be designed carefully to realize efficient photocatalysis. For samples with 5 min deposition of TiO_2, the TiO_2 layer was not thick enough (only about 10 nm) for inducing sufficient electrons and holes although their recombination could be inhibited availably. On the other hand, for samples with 15 or 20 min deposition of TiO_2, the TiO_2 layer was too thick (much more than 100 nm) that not only the light arrived at space charge layer was attenuated by excess TiO_2 but also the recombination was elevated in these TiO_2 because the TiO_2 layer might be thicker than space charge layer. In general, the optimal thickness for the photocatalysis was about 100 nm (depositing TiO_2 for 10 min). Consequently, about 100 nm of the TiO_2 layer was selected in the subsequent experiment.

3.2. Optimization of the deposition temperature and annealing temperature of TiO_2

Fig. 4 shows the XRD patterns of TiO_2–CNT heterojunction arrays with different annealing temperature. The peaks corresponded to graphite, TiO_2 and TiC reflection, respectively. The appearance of TiC peaks revealed the existence of a TiC layer between the Ti substrate and the bottom of CNTs [20]. In our fabrication process, CNT arrays began to grow on Ti substrate at 800 °C, and at this temperature, Ti is easily to form covalent bond carbide with CNTs according to titanium–carbon binary phase diagram [26]. The formation of conductive TiC could remove the barrier from the CNT–Ti interface thus permitting electrons to pass through more easily [27,28]. In Fig. 4, the crystalline signals of anatase TiO_2 were enhanced with increasing of annealing temperature. But the temperature near or above 450 °C was not a advisable selection, because the CNTs had been annealed from 450 °C in the cooling down step of our fabrication process for the appropriate surface to connect with TiO_2, if the annealing temperature after TiO_2 deposition was higher than 450 °C, some carbon at the TiO_2–CNT interface would be further removed and impaired the connection between the CNTs and TiO_2.

Jokiniemi and coworkers [29] investigated the chemical vapor deposition (CVD) process of TTIP, and they found the morphology of the deposits was very different depending on the deposition temperature. In this work, diffusion-controlled CVD took place at 320 °C resulting in the formation of the small nanoparticles, which could diffuse easily into the space between each CNT. With the increase of the deposition temperature, the TiO_2 nanoparticles with big size were produced and increased gradually in the gas phase. They assembled together and tampered the diffusion of TiO_2 into the space between each CNT, that is to say, the nanostructure films with incorporated particles would be formed on the CNT array surface instead of on the wall of each CNT.

According to the above discussion, the deposition temperature and annealing temperature of TiO_2 in the following experiments was 320 and 430 °C, respectively, for taking full advantage of the heterojunction arrays.

3.3. Superior mode for charge transfer

TiO_2–CNT heterojunction arrays with optimal conditions could provide a different mode of electrons transfer from aligned simplex TiO_2, such as TiO_2 nanotube arrays. In a TiO_2 nanotube, most TiO_2 nanoparticles are far away from the electron-collecting substrate (electrode), and photogenerated electron in one TiO_2 particle must hop or tunnel through too many boundaries from one TiO_2 conduction band to another until it finally enters the electrode that has a limited surface area (Fig. 5(a)), therefore most electrons will recombine with holes presenting in other TiO_2 particles. However, the TiO_2–CNT heterojunction arrays would provide more advantages because of the different mode of electrons transfer, as shown in

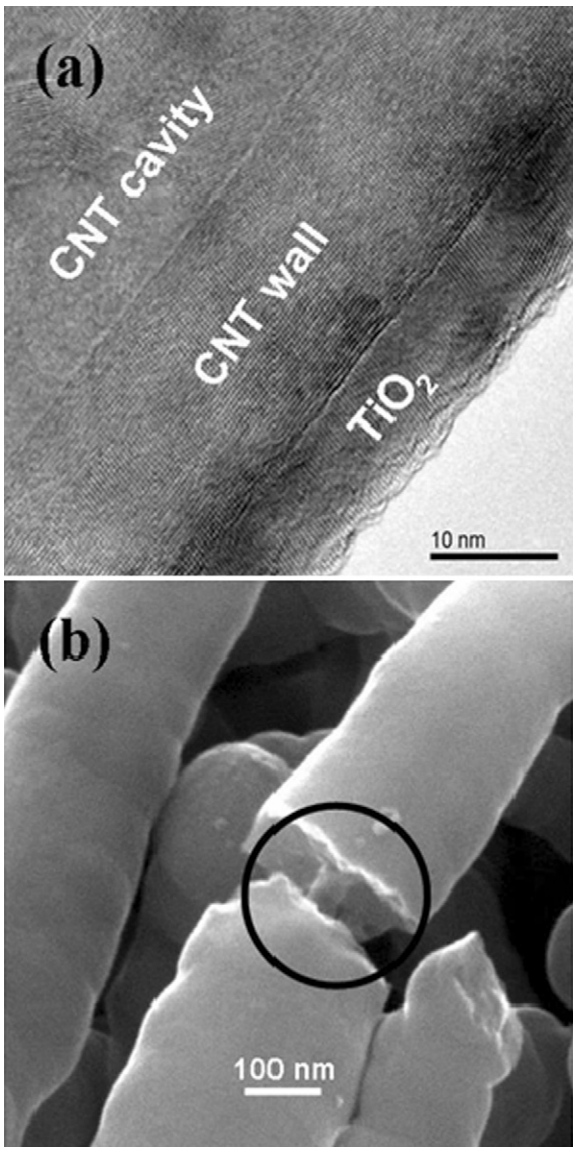

Fig. 2. TEM image of (a) TiO_2–CNT heterojunction with depositing TiO_2 for 5 min and (b) SEM image of TiO_2–CNT heterojunction with depositing TiO_2 for 10 min.

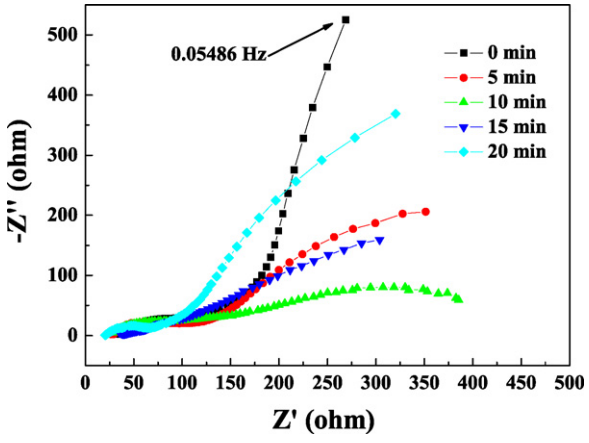

Fig. 3. Nyquist diagrams (Z'' vs. Z') of TiO_2–CNT heterojunctions with different TiO_2 deposition times under UV illumination.

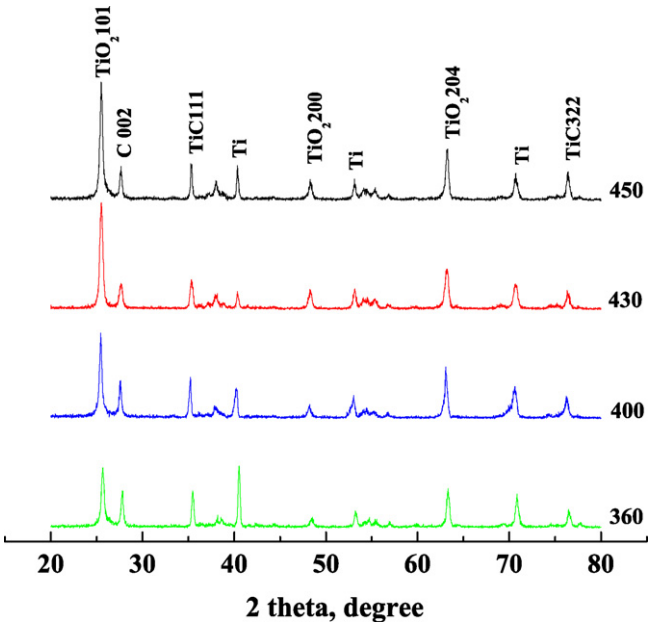

Fig. 4. XRD patterns of TiO_2–CNT heterojunctions on Ti substrate with different annealing temperatures.

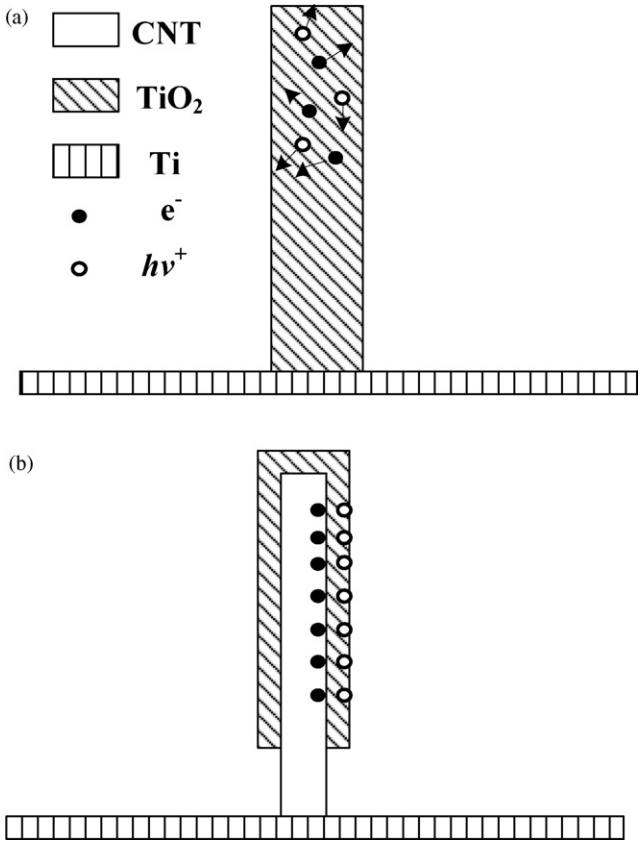

Fig. 5. Schematic diagram of electron transfer in (a) TiO_2 nanotube and (b) TiO_2–CNT heterojunction.

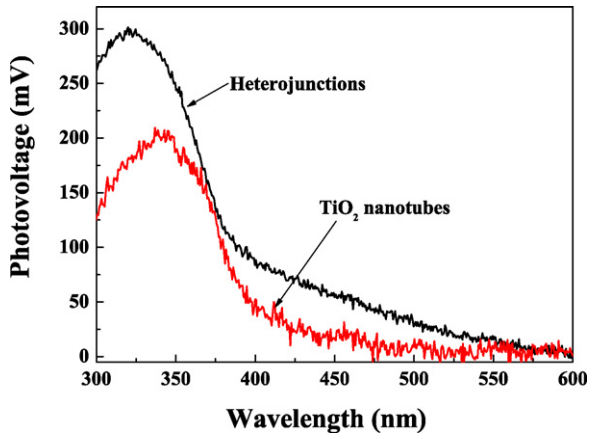

Fig. 6. SPV spectra of optimized TiO_2–CNT heterojunctions and TiO_2 nanotubes with top illumination taken on KP. (The data had been normalized.)

Fig. 5(b). The thickness of TiO_2 layer in heterojunctions approaches the space charge layer, therefore photogenerated electrons and holes could be separated by electrostatic force and the separated electrons transport into other semiconductor or metal rather than TiO_2. Consequently, the recombination would be inhibited.

3.4. Photoresponse in the air or in the solution

SPV is a well-established technique for the characterization of semiconductors, mainly reflecting the carrier separation and transfer behavior with the aid of light [30]. The signal of photovoltage is attributed to the changes of surface potential barriers before and after illumination, and the changes are modulated by the separation of photogenerated hole–electron pairs. Fig. 6 displays the surface photovoltage spectra of the TiO_2–CNT heterojunctions and TiO_2 nanotubes. For TiO_2–CNT heterojunctions, a positive SPV response ranged from 550 to 300 nm, which was broader than that of TiO_2 nanotube. The surface photovoltage signal of heterojunctions was stronger than that of TiO_2 nanotubes over the whole tested wavelength range, suggesting that a high photocatalytic activity could be expected for TiO_2–CNT heterojunctions.

Fig. 7 shows the Nyquist plots of TiO_2–CNT heterojunctions and TiO_2 nanotubes. The arcs of both heterojunctions and TiO_2 nanotubes were very big in dark, which indicated that there were few electrons across the TiO_2–electrolyte interfaces. While under the UV illumination, the arc of heterojunctions was much smaller than

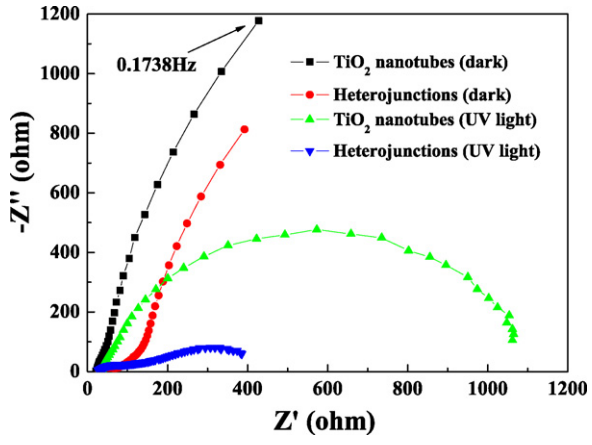

Fig. 7. Nyquist diagrams (Z'' vs. Z') for TiO_2 nanotubes and TiO_2–CNT heterojunctions in dark or under UV illumination.

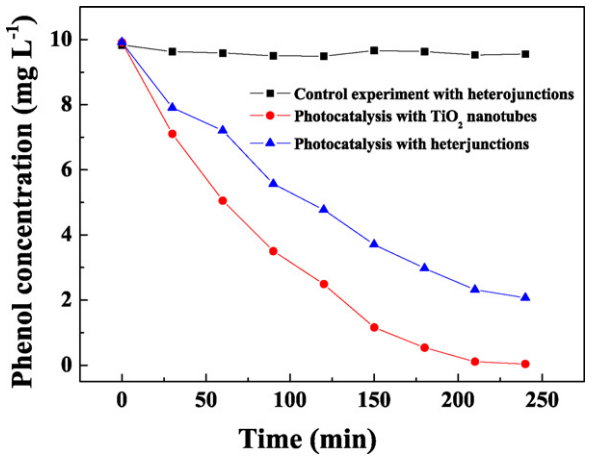

Fig. 8. Degradation of phenol under UV illumination (2.0 mW cm^{-2}) with TiO_2 nanotubes and optimized TiO_2–CNT heterojunctions.

that of TiO_2 nanotubes. EIS analysis illuminated that TiO_2–CNT heterojunctions displayed a smaller resistance than TiO_2 nanotubes at the TiO_2–electrolyte interface.

3.5. Photocatalytic abilities

As shown in Fig. 8, the experiments of photocatalytic degradation of phenol using TiO_2 nanotubes and TiO_2–CNT heterojunctions were carried out. As a control experiment, the degradation of phenol in dark with the TiO_2–CNT heterojunctions (connected with a platinum foil by a voltaic wire) was also performed, and the result indicated that phenol was very stable without UV light irradiation and the adsorption on TiO_2–CNT heterojunctions could be negligible. Under UV light irradiation, in 4 h, the degradation efficiency of phenol in photocatalytic process was up to 99.1% involving heterojunctions, whereas it was 78.7% on TiO_2 nanotube photoanode. The phenol degradation followed the pseudo-first-order kinetics, and the kinetic constants involving TiO_2–CNT heterojunctions and TiO_2 nanotubes were 0.75 h^{-1} (R^2 = 0.983) and 0.39 h^{-1} (R^2 = 0.995), respectively. The kinetic constant with this heterojunction arrays was 1.92 times as great as the value with the TiO_2 nanotube arrays.

The intermediate products during the phenol degradation were also detected (Fig. 9). The concentration of hydroquinone and benzoquinone (main ring intermediates from phenol oxidation [31]) kept increasing using the heterojunctions until 90 min, and then

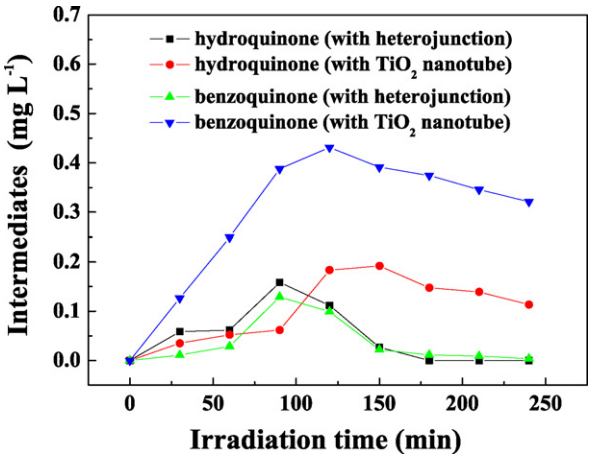

Fig. 9. Concentration of intermediate products during the phenol degradation.

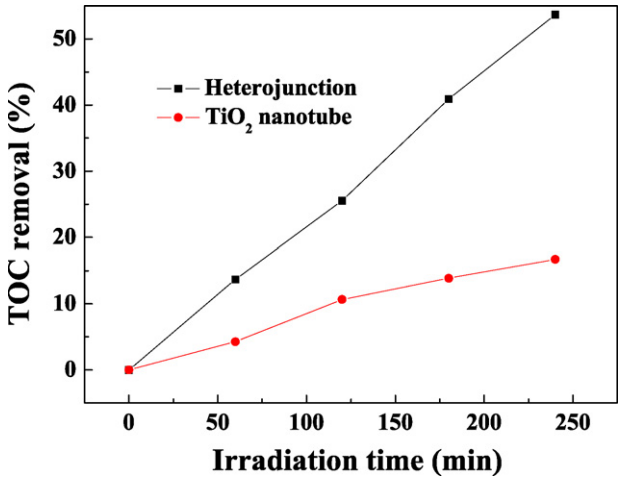

Fig. 10. The TOC removal of phenol with TiO_2 nanotubes and TiO_2–CNT heterojunctions.

decreased during 90–180 min. After 180 min, both hydroquinone and benzoquinone were completely degraded. Whereas using the TiO_2 nanotube arrays, the concentration of intermediate products increased quickly during the initial 90 min, and then intermediate products were decomposed slowly. This phenomenon indicated that the intermediate products of phenol degradation were subsequently oxidized rapidly by heterojunction anode, but accumulated in the solution with TiO_2 nanotubes.

To further illuminate the photocatalytic ability of TiO_2–CNT heterojunctions, the TOC was measured and shown in Fig. 10. In 4 h, 53.7% of TOC was removed with TiO_2–CNT heterojunctions and 16.7% with TiO_2 nanotubes, respectively. The TOC removal of TiO_2 nanotubes was less than that of heterojunctions, because considerable intermediate products were accumulated at the end of photocatalytic experiment using TiO_2 nanotubes. The result confirmed that the TiO_2–CNT heterojunction arrays possessed a higher mineralizing ability than the TiO_2 nanotube arrays.

4. Conclusions

As a key factor for enhancing the photocatalytic ability of TiO_2–CNT heterojunction arrays, the thickness of the TiO_2 layer could be controlled by varying the deposition time of TiO_2. In a photocatalytic system involving the TiO_2–CNT heterojunction arrays, the separated electrons could be driven by electrostatic field of space charge layer and flow into counter electrode simply using a thin voltaic wire connected between the working electrode (TiO_2–CNT heterojunction arrays) and the counter electrode without applying the external bias, and the holes might accumulate on the surface of the working electrode and lead to oxidative reactions. As a result, the TiO_2–CNT heterojunction arrays showed much better photocatalytic capability than that of TiO_2 nanotube arrays. Such a material is foreseen its potential application in removal of wide spectra of toxic organic pollutants from water due to its good photocatalytic capability in TOC removal.

Acknowledgments

This work was supported by National Nature Science Foundation P.R. China (No. 20337020) and the National Science Fund for Distinguished Young Scholars of China (No. 20525723). The authors would like to thank Prof. Dejun Wang and Dr. Qidong Zhao (Jilin University, China) for the SPV determination.

References

[1] M.R. Hoffmann, S.T. Martin, W. Choi, D.W. Bahnemann, Chem. Rev. 95 (1995) 69–96.
[2] A.L. Linsebigler, G.Q. Lu, J.T. Yates, Chem. Rev. 95 (1995) 735–758.
[3] T. Berger, M. Sterrer, O. Diwald, E. Knözinger, J. Phys. Chem. B 109 (2005) 6061–6068.
[4] Y. Chen, J.C. Crittenden, S. Hackney, Environ. Sci. Technol. 39 (2005) 1201–1208.
[5] E.V. Skorb, E.A. Ustinovich, A.I. Kulak, D.V. Sviridov, J. Photochem. Photobiol. A 193 (2008) 97–102.
[6] Z. Liu, D.D. Sun, P. Guo, J.O. Leckie, Nano Lett. 7 (2007) 1085–1801.
[7] T. Tatsuma, S. Saitoh, P. Ngaotrakanwiwat, Y. Ohko, A. Fujishima, Langmuir 18 (2002) 7777–7779.
[8] X. Fu, L.A. Clark, Q. Yang, M.A. Anderson, Environ. Sci. Technol. 30 (1996) 647–653.
[9] R. Brahimi, Y. Bessekhouad, A. Bouguelia, M. Trari, J. Photochem. Photobiol. A 186 (2007) 242–247.
[10] W. Siripala, A. Ivanovskaya, T.F. Jaramillo, B.S. Hyeon, E.W. McFarland, Sol. Energy Mater. Sol. Cells 77 (2003) 229–237.
[11] Y. Bessekhouad, D. Robert, J.V. Weber, Catal. Today 101 (2005) 315–321.
[12] Y. Yu, J.C. Yu, C.Y. Chan, Y.K. Che, J.C. Zhao, Lu. Ding, W.K. Ge, P.K. Wong, Appl. Catal. B 61 (2005) 1–11.
[13] X.H. Xia, Z.J. Jia, Y. Yu, Y. Liang, Z. Wang, L.L. Ma, Carbon 45 (2007) 717–721.
[14] W. Wang, P. Serp, P. Kalck, J.L. Fari, Appl. Catal. B 56 (2005) 305–312.
[15] A. Kongkanand, R.M. Domínguez, P.V. Kamat, Nano Lett. 7 (2007) 676–680.
[16] H. Huang, W.K. Zhang, X.P. Gan, C. Wang, L. Zhang, Mater. Lett. 61 (2007) 296–299.
[17] Y. Yang, L. Qu, L. Dai, T.S. Kang, M. Durstock, Adv. Mater. 19 (2007) 1239–1243.
[18] S. Orlanducci, V. Sessa, M.L. Terranova, G.A. Battiston, S. Battiston, R. Gerbasi, Carbon 44 (2006) 2839–2843.
[19] H.T. Yu, H.M. Zhao, X. Quan, S. Chen, Chin. Sci. Bull. 51 (2006) 2294–2296.
[20] H. Yu, X. Quan, S. Chen, H. Zhao, J. Phys. Chem. C 111 (2007) 12987–12991.
[21] X. Quan, S. Yang, X. Ruan, H. Zhao, Environ. Sci. Technol. 39 (2005) 3770–3775.
[22] J. Marsh, D. Gorse, Electrochim. Acta 43 (1998) 659–670.
[23] A. Zaban, A. Meier, B.A. Gregg, J. Phys. Chem. B 101 (1997) 7985–7990.
[24] F.F. Santiago, G.G. Belmonte, J. Bisquert, A. Zaban, P. Salvador, J. Phys. Chem. B 106 (2002) 334–339.
[25] H. Liu, S. Cheng, M. Wu, H. Wu, J. Zhang, W. Li, C. Cao, J. Phys. Chem. A 104 (2000) 7016–7020.
[26] C.P. Deck, K. Vecchio, Carbon 44 (2006) 267–275.
[27] Y. Zhang, T. Ichihashi, E. Landree, Science 285 (1999) 1719–1722.
[28] J. Zhang, X. Wang, W. Yang, Carbon 44 (2006) 418–422.
[29] U. Backman, A. Auvinen, J.K. Jokiniemi, Surf. Coat. Technol. 192 (2005) 81–87.
[30] L. Kronik, Y. Shapira, Surf. Sci. Rep. 37 (1999) 1–206.
[31] F. Mijangos, F. Varona, N. Villota, Environ. Sci. Technol. 40 (2006) 5538–5543.